

Shape-programming Robotic Reflectors for Wireless Networks

Yawen Liu, Akarsh Prabhakara, Jiangyifei Zhu, Shenyi Qiao, Swarun Kumar

Abstract—With the increasing use of wireless technologies in robotics for communication, sensing, and localization, the potential benefits of how robotics can complement and enhance wireless systems remain underexplored. This paper explores a novel application of the existing inflatable robots for wireless communication systems by forming a shape-programming, reflective waveguide that enhances the received signal quality for wireless devices. Our primary target is enhancing Low-Power Wide-Area Networks (LP-WANs) – where 10-year battery-powered client devices (e.g. energy meters or smart home sensors) connect to cellular-like base stations to deliver data. Devices in these networks often experience significant seasonal variability in battery life – even simple obstructions between the device and base station (e.g. due to construction) can shave off years of battery life. We propose MetaMorph, a programmable robotic reflector attached to base stations that enhances signal quality from client devices by enhancing received signal energy with controlled reflections. We investigate the design of the reflector, and our experiments show the ability to improve the signal quality for LP-WAN (LoRa) communication systems demonstrating signal quality and battery-benefits. To our best knowledge, MetaMorph is the first paper to explore how flexible robotics can serve as virtuous reflectors for wireless communication systems.

I. INTRODUCTION

Robots carry a variety of wireless sensors and communication devices to perform complex tasks such as grasping, perception, and control. In fact, examples of wireless systems that improve robotics are numerous: low-power connectivity for multi-robot collaboration [1], [2], [3], high-resolution radar imaging [4], [5], [6], and wireless actuated battery-free robots [7], [8], [9], [10]. In contrast, the question of how robots can benefit wireless technologies is relatively less explored. This paper draws on advances in soft robotics to address a key performance problem in an important class of wireless networks – Low-Power Wide-Area Networks (LP-WANs), specifically Long-Range (LoRa) communications.

LoRa is a technology that offers long-range connections (several kilometers) to low-power (10-year battery-powered) devices such as energy meters, occupancy sensors, and other Internet of Things devices. Due to the longer wavelength of the LoRa devices, their signal can travel further away with less power decay. However, their signal propagation still encounters reflection, refraction, and interference such as other Radio Frequency (RF) waves. Environmental changes, such as construction sites, foliage, or temporary blockages

Y. Liu, J. Zhu, S. Qiao, S. Kumar are with the Department of Electrical and Computer Engineering, Carnegie Mellon University, Pittsburgh, PA 15213 USA. A. Prabhakara is with the Department of Computer Sciences, University of Wisconsin-Madison, Madison, WI 53706 USA yawenl@andrew.cmu.edu, akarsh@cs.wisc.edu, {jiangyiz, shenyiq}@andrew.cmu.edu, swarun@cmu.edu

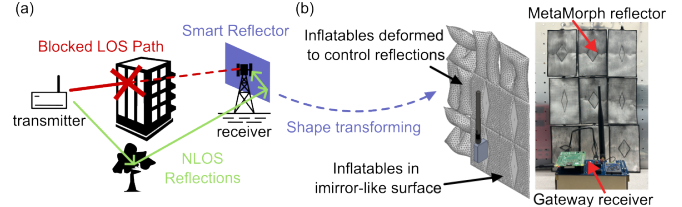


Fig. 1: MetaMorph surface backscatter radiated power, leveraging the shape-programming robots to alter the direction of the reflected paths toward the receiving antenna.

introduce signal multipaths, which can severely degrade the signal-to-noise ratio (SNR) of the transmissions from the client devices to the base stations. These changes in signal multipaths can result in significant SNR degradation [11] driving the anticipated battery life of a user device from several years to a few months.

Indeed, much prior art exists on LP-WAN coverage enhancement [12], [13], [14], [15], yet requires denser and more complex base station hardware. In this paper, we consider strategically placing RF reflectors around the base station that are designed and controlled to enhance received signal quality. These add additional signal paths that superimpose constructively at the base station, enhancing client signal quality. Rich prior work exists on manipulating wireless propagation through passive reflectors [16], [17], [18], [19] and more recent meta-material surfaces [20], [21], [22], [23], [24], primarily at WiFi (2.4/5 GHz) and mmWave bands (10s of GHz). However, what these systems lack is the ability to remain highly compact at 900 MHz LoRa bands (reflector surface increases as wavelength increases with LoRa wavelength at 32.7cm) and programmable to adapt to changes in the environment.

This paper investigates how shape-changing robots can inspire new RF reflector designs for signal enhancement. We propose MetaMorph, the first shape-programmable device to our best knowledge, building on the interdisciplinary study between shape-programming robots and wireless smart surfaces to enhance signal reception. MetaMorph is an inflatable-robot-based *passive smart reflector* attached to the LP-WAN base stations enabling programmable wireless coverage. Our system is, to the best of our knowledge, the first programmable reflector design for LP-WAN systems.

MetaMorph's core is to create a surface with programmable ridges or hills that create beneficial reflected signals, utilizing the multipath from the environment. As illustrated in Fig. 1(a), the reflective robotic surface utilizes the non-line-of-sight (NLOS) signals from the environment to create virtuous signals focused on the receiver when the line-of-sight (LOS) signal path is blocked. Specifically,

we envision an RF reflector that can mechanically deform into different shapes and offer virtuous paths that constructively interfere with the environment at the receiving antenna. Specifically, MetaMorph comprises an array of robotics programmable reflectors to mitigate radiation energy lost due to a blocked LOS and multipath propagation, as shown in Fig. 1(b). If the propagation effects change in the scene, MetaMorph measures SNR information under shape deformation’s impacts and infers an optimal configuration without knowing the environment.

In designing MetaMorph, we encountered two main challenges. First, the reflector structure needs to be shape-programmable to address multipath dynamics. Multipath interference occurs when multiple radio signals arrive at the receiver and cancel each other because of signals bouncing off from objects. Thus, fixed passive reflectors cannot adapt to changing environmental factors, which is why we must configure reflector geometry in a controlled manner. MetaMorph’s reflector is therefore designed to reprogram itself to optimize signal reflections based on signal strength variation. If the signal strength drops significantly due to blockage or foliage, MetaMorph searches through a combination of shapes for best signal reception.

A second challenge in MetaMorph is to achieve a design with minimized surface area. Particularly, if we adapt metamaterial surface design from [20], an estimated surface area of 3 tiled surfaces $\times 50\text{cm} \times 60\text{cm}$ is required for LP-WANs. In contrast, off-the-shelf LP-WAN devices have a package smaller than $15\text{cm} \times 15\text{cm} \times 3\text{cm}$. Designing a smaller reflector surface that is compatible with easy deployment is crucial. To address this, we observe that rough surfaces can diffuse or focus the reflected path even with a smaller surface area if placed in the near field, that is close to the base station antenna. MetaMorph leverages this observation to design and program roughness as defined by signal wavelength to provide beneficial reflections from a compact surface.

We design and implement MetaMorph with reflector components controlled by a microcontroller, pumps, and air valves to adjust the inflation. We fabricate the designed reflective robotic elements using an elaborate process (design and simulation will be made open source). MetaMorph’s evaluation reveals an average gain of 2.35 dB in SNR for 915 MHz LoRa. We demonstrate this is equivalent to 89.68% battery-life improvement for LoRa client devices.

Contributions: MetaMorph propose a novel soft robotic design that enables virtuous signal reflection controls for wireless communication systems. To our best knowledge, MetaMorph is the first inflatable-robot-based system used for RF reflector design. We implement MetaMorph on commercial, wireless devices to demonstrate how robotic-controlled reflectors enable signal strength enhancements, throughput improvements, and battery life benefits.

II. RELATED WORK

Robotics for RF: Prior work has developed flexible antennas that utilize the mechanical shelving of metals and inflatables for antenna frequency tuning [25]. In contrast,

MetaMorph leverages pneumatically actuated soft robots to improve signal quality through virtuous reflections, using cheaper, simpler hardware and more variety in shape-shifting mechanisms [26], [27], [28], [29]. Inflatables have many advantages in being lightweight, safe, and low-cost, enabling shape customization with a high degree of flexibility [26], [30]. Rather than motor-based and heat-based actuation that incurs bulkiness and longer latency [7], [31], [32], [33], MetaMorph builds on inflatable soft robots, exploring a unique application for wireless systems.

Reflectors, Waveguides and Smart Surfaces: Reflectors can enhance wave propagation in microwave and optical networks [16], [17]. Traditional metal reflectors can passively disentangle signal paths or form standing wave patterns, with geometry dramatically affecting performance. Advances in 3D printing and RF propagation modeling improve the design procedure of passive reflectors [18], [19]. However, once fabricated, they cannot adapt to real-world changes such as seasonal landscapes, moving furniture, or temporary construction. MetaMorph complements this limitation by enabling geometry programming.

Prior work has also proposed programmable RF smart surfaces. These are specialized reflectors with antenna elements to control signal reflections using phase shifters, RF switches, or mechanical switches [34], [35], [36], [37], [20], [38], [39]. Although such surface designs are well studied for low frequencies (sub-kilo-Hz to 20MHz) and high frequencies (5GHz to sub-THz) [20], [21], [22], [23], [24], efficient designs for the LP-WAN bands (~ 900 MHz) remain comparatively scarce owing to large form factor (surface area usually in tens of wavelengths). In contrast, we utilize inflatable robots for better deployment flexibility, leveraging their lightweight and small form factor to reduce system bulkiness by at least 5 times.

Wireless Networks: LP-WAN literature includes a variety of robust coverage enhancement techniques such as mesh networks, distributed gateways and repeaters, and reinforcement learning-based parameter tuning [40], [15], [41], [42], [43], [44]. Power optimization algorithms can reallocate resources to minimize signal interference to increase reception SNR [45], [46], [22]. Instead, MetaMorph explores improvements in link quality through shape-shifting reflectors that add virtuous multipaths at the base station without requiring additional hardware or energy burden to clients.

III. METAMORPH SYSTEM DESIGN

MetaMorph is composed of shape-shifting soft robotic platforms that program wireless coverage, adapting to quasi-static environmental changes. We first study the design space of MetaMorph shape-programming robot that can be precisely controlled. Each robot is an airbag that deforms, undergoing inflation and deflation. We evaluate the shape-changing robots and explore how they collaboratively enable signal reflection by forming RF “roughness”, through careful modeling of how soft robots interact with the RF propagation. In this section, we detail the shape-programming

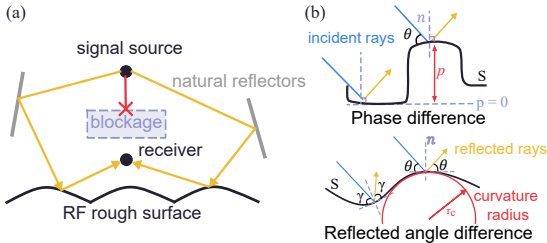


Fig. 2: Understanding how to model and control the RF roughness in terms of heights and curvature

mechanism, the reflector robot's dimension, the placement of the robots, fabrication, and an actuation system.

A. Designing Soft Robotic Elements

This section discusses how the design of shape-changing elements affects RF waves and causes differences in signal strength. MetaMorph arranges multiple shape-changing robots together into a shape-changing *surface* that influences RF propagation.

Shape-changing Mechanism: Prior work in pneumatically controlled soft robots utilizes heat-sealed structures that guide airflow to deform airbags into particular shapes [27], [47], [48]. The simplest pneumatic control system with a vacuum pump to supply the airflow and two valves to direct the flow. This setup manages the airflow in and out of a single airbag with three operational modes: inflate, deflate, and lock. The pump can either inflate/deflate air flow, the first valve stops/supplies the airflow to the second valve, and the second valve closes/opens the flow to the airbag. We design the sealed patterns of the airbags for geometry changes.

Engineering RF scattering: Electromagnetic (EM) waves deflect in different directions when interacting with a surface. When these interactions happen at objects smaller or comparable to a wavelength, the energy disperses in all directions. This phenomenon is known as Rayleigh scattering, where the surface's height variations and curvature affect the scattered energy distribution [49], [50]. Due to the Rayleigh scattering, the MetaMorph reflector robot can program EM waves with a small surface area if its dimension is about sub-wavelength. A reflector smaller than this limit is ineffective, as most of the energy will bypass, resulting in inadequate signal enhancement. Depicted in Fig. 2(a), MetaMorph creates an *RF rough surface* with a bumpy texture, where the microscopic area is oriented differently, increasing the likelihood of energy being backscattered towards the receiving antenna for improved link quality.

Changes in height and curvature influence two RF properties: RF phase and reflected waves' direction (Fig. 2(b)). Height variations induce phase shifts between signal rays that travel different distances, while the Rayleigh Scattering Criteria calls a surface rough if the phase difference is significant ($> \pi/2$). Thus, a scattering surface must have a comparable height difference $p > \frac{\lambda}{8\sin(\theta)}$ (4 cm at 915 MHz) at two interaction points, where λ is the wavelength and θ is the incident angle to the surface tangent. Meanwhile, the curvature size must not be too small compared to wavelengths to avoid sharp edges and undesired diffraction.

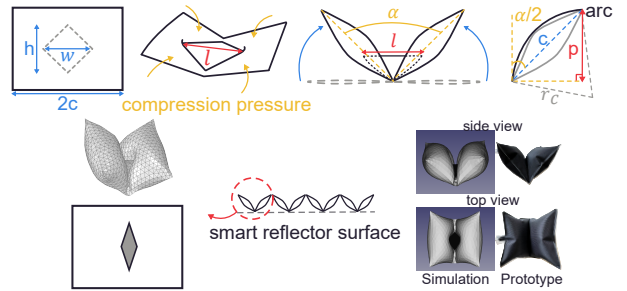


Fig. 3: The geometries and mechanisms of the deforming robots (top); an example of shape-changing reflector simulation and prototype (bottom)

We base local curvatures using Brekhovskikh's geometry definition, which specifies the principal radius of curvature r_c should follow $4\pi r_c \sin(\theta) > \lambda$ to eliminate diffraction [49]. We calculate that the curvature's principal radius must be over 9.84 cm at the near-grazing incidence (15°) and exceed 2.55 cm at the orthogonal incidence (90°).

Shape-programming Parameters: MetaMorph's robot leverages bending as its shape-shifting mechanism based on prior work [26] – inspired by the concept of corner reflectors, where multiple surfaces form an L-shape corner to focus radio signals. We explore the dimension of each discrete robot that satisfies the RF roughness to effectively reflect EM waves, characterized by its air-tight hinge parameters (the shaded area in Fig. 3) and outer dimensions (denoted $2c$). The rigid hinge pattern blocks airflow, creating side pressure that folds the airbag, as shown in Fig. 3. We then choose the hinge patterns (denoted $w : h$ ratio) and adjust the inflation levels to achieve height and curvature variations.

Dimension of a Single Reflector Robot: Let's now build a geometry model of inflatable robots with length l (could vary due to inflation) and the bending angle: $\alpha = \text{acos}(1 - \frac{2w^2}{l^2})$ [26]. In Fig. 3, we consider $r_c \approx \frac{c}{2\sin(\frac{\alpha}{2})}$ and $p = c \times \cos(\frac{\alpha}{2})$; where c is one half the element's outer dimension. We choose $2c$ as 12 cm to satisfy RF roughness constraints. We experimentally choose two w values along the shorter reflector edge and explore five h values, in multiples of 1.5 cm ($\approx \lambda/20$). We use Rhinoceros 3D to build physical models of robot-inflating (Fig. 3). The prototypes with their corresponding designs and maximum bending angles are shown in Fig. 4. Fig. 5 compares our CAD simulation and measurements of the fabricated inflatables with consistent geometry, ensuring height and curvature compliance.

B. Modeling Reflected Power

Thus far, we have shown how MetaMorph enables programming RF roughness. Next, we analyze the EM wave interactions on the reflector robot and combine multiple robots to focus the reflected signals.

Impacts of Hinge-patterns, Inflation, and Placement: Building on the mathematical model of RF scattering in Sec. III-A, we now perform EM wave simulations to study the reflected power with three key properties: (1) the element's hinge $w : h$ ratio; (2) the inflation level; (3) positioning of MetaMorph reflector to the antenna. We input

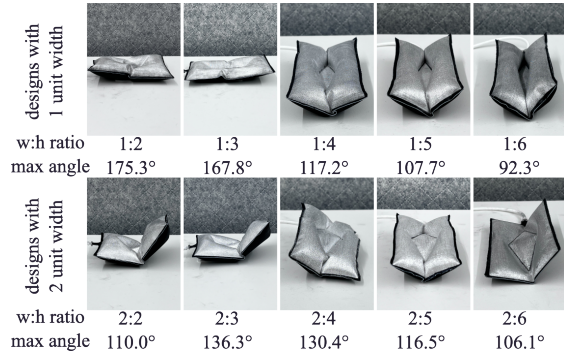


Fig. 4: MetaMorph robots and their maximal bending angles.

by seams.pdf

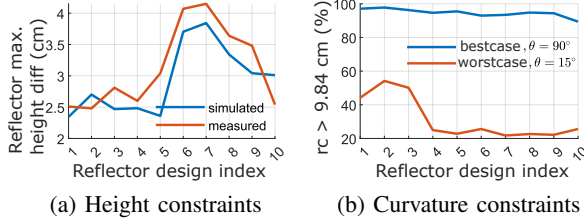


Fig. 5: MetaMorph robots' considerations of RF roughness

the CAD models of reflector robots to Ansys HFSS and SBR+ solvers and explore their reflected radiation patterns. Fig. 6 shows the reflected radiation under various hinge patterns and inflation levels along the azimuth and elevation axes. The inflation level dominates the reflection radiation distribution along the azimuth, while the hinge pattern affects both axes. Then, we evaluate reflector positioning using the S11 parameter reflectivity coefficient to measure the reflected power. We placed a single reflector robot, inflated to its highest gain (denoted P_o), near a 915 MHz omnidirectional antenna connected to a Keysight N9916A vector network analyzer. Our findings reveal two key points: (1) MetaMorph reflector provides inherently wideband gain since the S11 reflectivity shows negligible frequency shift (Fig. 7); (2) the closer the reflector is to the antenna, the higher the calculated gain (Fig. 8). The placement distance, d_0 , affects the gain that drops proportionally to $1/d^4$, consistent with the near-field propagation distance($< 2 \times \text{reflector size}^2/\lambda$) [51], with a highest 1.005 gain that diminishes further away.

Combining Multiple Reflector Robots: To effectively combine multiple reflector robots, we develop a numerical model to estimate the signal strength using the Friis transmission formula [52]. We assume that the individual reflector robots each contribute the highest gain after inflation control. Let $P_i = P_0 d_0^4 / d_{\text{new}}^4$ denote the new power gain contribution for each displaced robot compared to the measurements in Fig. 8. We calculate the total reflective power, $P_{\text{total}} = (\sum_{i=1}^N \sqrt{P_i})^2$, with N elements that make up the surface. We use this framework to find the highest possible signal strength in Fig. 9 (the signal strength measurement without a reflector is -100 dBm). Based on this analysis, we choose a 4-element reflector placed 5 cm behind the receiving antenna. Note that multiple robotic elements increase gain; they also increase form factor. Our choice of 4-elements serves as a

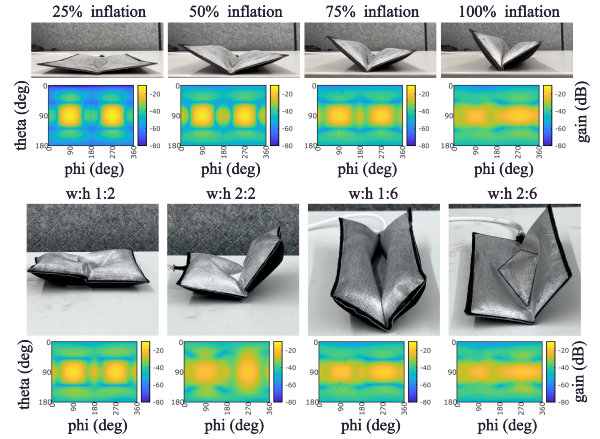


Fig. 6: Reflected radiation of different inflation levels (top) and air-tight hinge (bottom)

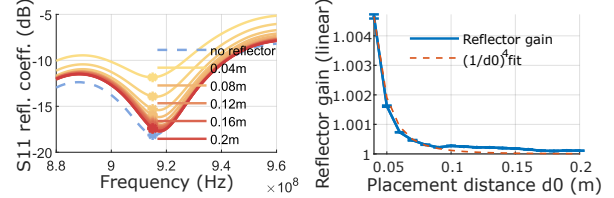


Fig. 7: S11 measurements

Fig. 8: Reflector gain

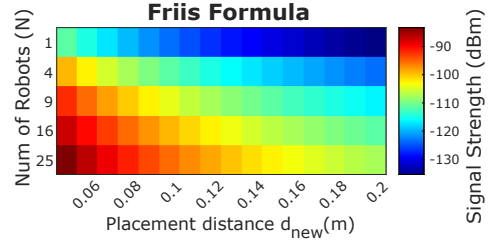


Fig. 9: Signal strength vs. sizes and distances

good compromise in this trade-off.

Radiation Pattern Optimization: After obtaining the reflected radiation of a single reflector robot in Fig. 6, we optimize the arrangement of hinge patterns for our 4-element MetaMorph surface. However, a 2×2 reflector-units surface can provide 10^4 arrangements with 10 different pre-fabricated hinge patterns. To reduce simulation overhead, we synthesize the normalized field distribution using the vector sum technique [53]. We estimate the total reflected power from N -robots as $[\sum_{n=1}^N \sqrt{\sigma_n} \exp(\frac{j4\pi d_n}{\lambda})]^2$, where σ_n is the reflected radiation of a single reflector robot, displaced d_n from the antenna. Among all reflected radiation in Fig. 10, we choose the hinge pattern combination of 1:4, 1:6, 2:2, and 2:6 for maximum gain in Fig. 11, when the reflector is placed behind the receiving antenna and the targeted enhancing area is the 90-degree sector in front of the receiver.

C. Fabrication

Inflatable Robotic Airbag Fabrication: We fabricate the reflector robots by heat-sealing two layers of thermoplastic polyurethane (TPU) fabric with an air nozzle opening [54], [48], [26]. We attach a soldering tool to the Genmitsu 3018-PRO CNC router machine controlled by G-code from Auto CAD and Inkscape, to seal the air-tight hinges and outer

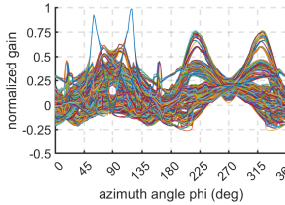


Fig. 10: Radiation patterns

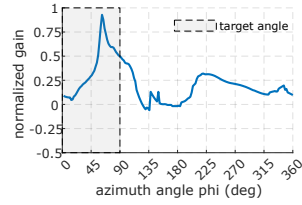


Fig. 11: Optimal pattern

boundary. Each robot is connected by a plastic pipe connector and two heat-sealable 200D Oxford fabrics ($\leq \$0.40$ each), including typesetting costs. Minor fabrication errors that may cause irregular buckling (Fig. 4), albeit are negligible in performance impact as the fabrication errors remain much smaller than the sub-wavelength scale.

Choice of Reflective Coating: The MetaMorph robots must be reflective, i.e. with good conductivity for EM wave reflections. While rigid metals, aluminum foil, and conductive sprays offer limited flexibility, we apply a thin layer of eutectic gallium-indium (EGaIn) [55], [56], [57], a liquid metal alloy, to the TPU robotic units to achieve a uniform, glazed surface. This maintains the MetaMorph robots' plasticity and flexibility to endure inflate-deflate cycles. Using effective medium theory (EMT) test [57], we verify EGaIn surface's reflection coefficient exceeds 0.91, indicates a good ratio of reflected-to-incident EM waves [58]. For comparison, a perfect reflector has a coefficient of 1, and copper has 0.89.

D. Control Architecture

Adaptive Inflation/Deflation Control: To effectively control MetaMorph robots for focusing EM energy on the antenna and enhancing signals, we propose a closed-loop feedback system that optimizes inflation level element-wise. Three of the four robots are kept flat (0%) and inflate one MetaMorph reflector robot from 0-100% inflation, which takes about 3 seconds. After identifying the inflation level for a local maximum received signal strength (RSSI), the robot deflates and reinflates to that level, compensating for inflation-deflation asymmetry. The process is repeated for all four reflector robots. While a local maximum RSSI is not always the global best configuration, we record the highest RSSI to determine a global optimal across all searches and install the final configuration. This control system relies on continuous RSSI monitoring at the gateway receiver, leveraging wireless communication channel state information. MetaMorph is configured actively based on periodic LoRa transmissions. This system iteratively updates using the RSSI feedback, adapting to long-term multipath changes.

Control actuation hardware: We use a customized driver PCB with a microcontroller for all MetaMorph robots by switching on/off valves at each element with two continuous inflating and deflating pumps. We assemble our reflector robots using multiple 2-valves control architecture as discussed in Sec. III-A. Figure 12 depicts the pneumatic actuation architecture: the first level air valve (highlighted in purple) selects an element during time-multiplexing and the second level air valve (highlighted in orange) switches the element's air between the inflating or deflating pump. Since

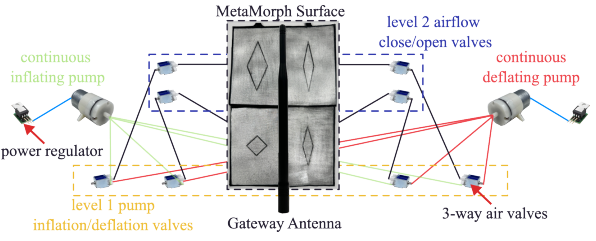


Fig. 12: Pneumatic actuation architecture

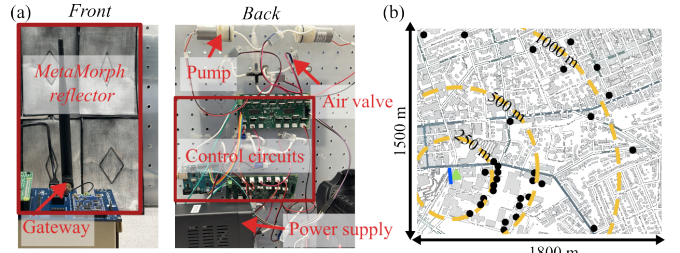


Fig. 13: MetaMorph with control hardware and testbed

LP-WAN clients transmit infrequently, our optimization process is not significantly constrained by latency. Given that LP-WAN packets are both long duration (up to seconds), transmitted infrequently (a few times a day), and often at predictable schedules (e.g. smart sensors). MetaMorph's adaptability is designed to be gradual and cognizant of long-time-scale changes across days and weeks when signal degradation is observed.

IV. EVALUATION

A. Evaluation Setup

System: We assemble inflation control tubes and MetaMorph platform with an Arduino Uno board, as shown in Fig. 13(a), with 15×25 cm surface area. MetaMorph reflector is placed behind the gateway receiver, and the reflective elements are mounted on a stationary platform to hold them in place.

Transmitter and Receiver: We deploy commodity Semtech SX1302 LPWAN gateway and SX1262 chip client devices for channel RSSI measurements to show SNR gains, with an emitting power of +22dBm and 1.5 dB Noise Figure. We compare the SNR gains to a smooth plate baseline reflector.

Testbed: We conduct tests at varied distances, with short/long-term environmental changes and chirp configurations, in a university campus and surrounding area of size 2.7 sq. km, as in Fig. 13(b) with these notations: MetaMorph **I**, the gateway **▲**, the clients **●**, the distance from the gateway **—**. The MetaMorph platform is co-located with a fixed transmitter and multiple quasi-static and dynamic receivers.

B. SNR Enhancement

Evaluation Methodology: We deploy the LoRa link at 30 locations as in Fig. 13(b), with a stationary client and the gateway under the same spreading factor (SF) and bandwidth (BW) of 7 and 125 kHz. For each link, MetaMorph finds the optimal configuration that maximizes RSSI. To mitigate signal fluctuations, we perform 60s measurements and present the average SNR with or without MetaMorph.

Result: MetaMorph achieves a median of 0.7 dB, 1.3 dB, and 4.1 dB SNR gains for different link distances at 1000

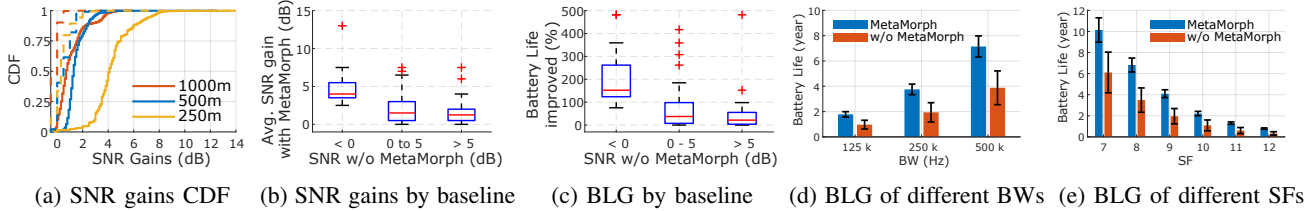


Fig. 14: Overall performance of MetaMorph for LP-WAN in Signal-to-Noise Ratio (SNR) and Battery Life Gain (BLG). The solid line and dashed line represent the performance of MetaMorph and the baseline rigid reflector, respectively.

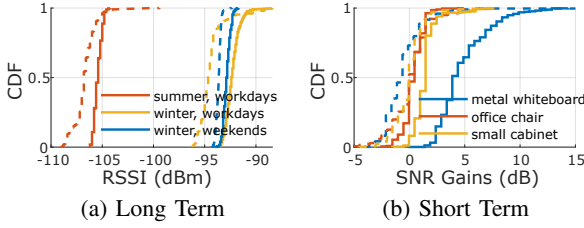


Fig. 15: SNR gain to various environmental changes

m, 500 m, and 250 m, respectively (Figure 14a). MetaMorph achieves an average of 2.35 dB gain of all locations, and 2.1 dB higher SNR gain than the baseline reflector, which validates the promise of controlling a rough scattering surface. To provide some intuition on how these gains compare to related prior art, a prior hardware-defined smart surface [20] achieves a median 2 dB gain for single antenna transceivers for 5 GHz Wi-Fi networks; while, software-defined techniques such as [59] achieve 1.84-2.35 dB gain and [60] achieves a median 3.16 dB gain for 200m-ranged 915 MHz LP-WAN. The results showcase MetaMorph’s performance in real-world multipath scenarios. MetaMorph works better to provide gains for originally weaker links, and the gain starts decreasing for LoRa nodes further away because MetaMorph reuses the multipath. For distant clients, the power of the multipath signals also drops inversely half to the distance between the transceivers.

C. Battery Life Improvements

Evaluation Methodology: We evaluate improvement in battery life gain (BLG) for the client device using the standard extended LoRa battery lifetime models [61], [60] in a setup akin to Sec. IV-B. The small SNR gain is valuable because a 3dB gain enables the LP-WAN device to reduce the SF by 1 and save an estimated 30% battery life [60].

Result: In Figure 14c, we evaluate the battery life benefits with an average of 89.68% improvement across links. We observe a median of 152.4%, 37.4%, and 21.6% battery life saved for the links originally without MetaMorph at low, median, and high SNR levels respectively, as shown in Figure 14(b-c). We investigate the battery life gain variations upon different bandwidth and spreading factor configurations in Figure 14(d-e) with an average of 1.78, 3.75, and 7.14 years for a baseline SNR of -2 dB. In comparison to baseline, MetaMorph extends the average battery life by 92.8%, 93.3%, and 84.0% for the three configurations. The battery life gain increases as the SNR decreases because a higher SF is usually preferred under a lower SNR level in Fig. 14(c), while MetaMorph SNR gains are significant to

lower the energy consumption for the new SF configuration. This matches our observation in Figure 14(e), where the battery life when using an SF=12 is less than 0.8 years, much smaller than that using SF=7 for 10.1 years.

D. Impacts of Environmental Changes

Evaluation Methodology: MetaMorph’s goal is to mitigate signal quality decay from environmental changes. We observe 10 dBm RSSI drops in different seasons, where the same link in summer is weaker than in winter because the lush foliage can significantly weaken the signals (Fig. 14d). We conduct long-term experiments that each of the five trials last 10 minutes, across seasons and weeks to verify the long-term impacts of furniture and seasons.

Result: MetaMorph continues to improve the channel quality with 2.1 dB, 2.4 dB, and 0.7 dB gains in the summer workdays, winter workdays, and winter weekends respectively. We also investigate how MetaMorph can balance the signal degradation due to short-term blockage (i.e. objects placed near gateway or client devices). We found introducing various blockages on the transceivers degraded signal by a median of -1.4 dB; MetaMorph continues enhancing the link by a median of 1.8 dB SNR gain in Fig. 15.

V. CONCLUSION AND FUTURE WORK

This paper explores MetaMorph, a novel shape-programmable reflector to improve the battery life of the client for LP-WANs – leveraging the shape-programming robotic reflectors co-located with the base station. We design soft pneumatic actuators that serve as programmable RF-rough surfaces to induce constructive RF scattering paths that enhance signal quality along the link from the client to the base station. We demonstrate how doing so significantly enhances the battery life of LoRa clients, which can drop quite significantly when signal quality to the base station is impacted. MetaMorph is specially designed to respond to changes in signal quality due to variations in the environment that result in long-term impacts, such as construction or changes in interior decor near the clients. We leave optimizing inflatable designs and extending MetaMorph to respond to more rapid environmental changes such as moving cars/humans to future work.

Acknowledgments: We acknowledge support from the NSF (2106921, 2030154, 2007786, 1942902, 2111751), ONR (N00014-24-1-2062), AFRETEC, MFI, CISCO, Safety21, and CyLab-Enterprise. Any opinions, findings, and recommendations expressed in this material are those of the authors and do not necessarily reflect the views of the above. We also thank Prof. Carmel Majidi and his student Mason Zadan, Prof. Lining Yao and her student Jianzhe Gu for their inputs.

REFERENCES

- [1] H. Wu, G. Tian, and B. Huang, "Multi-robot collaborative localization methods based on wireless sensor network," in *2008 IEEE International Conference on Automation and Logistics*. IEEE, 2008, pp. 2053–2058.
- [2] T. Andre and C. Bettstetter, "Collaboration in multi-robot exploration: to meet or not to meet?" *Journal of intelligent & robotic systems*, vol. 82, pp. 325–337, 2016.
- [3] S. Li, S. He, Y. Zhang, X. Shi, G. He, and T. Jiang, "Edge intelligence enabled heterogeneous multi-robot networks: Hybrid framework, communication issues, and potential solutions," *IEEE Network*, vol. 36, no. 6, pp. 108–115, 2022.
- [4] A. Prabhakara, T. Jin, A. Das, G. Bhatt, L. Kumari, E. Soltanaghai, J. Bilmes, S. Kumar, and A. Rowe, "High resolution point clouds from mmwave radar," in *2023 IEEE International Conference on Robotics and Automation (ICRA)*, 2023, pp. 4135–4142.
- [5] H. Chen, Y. Liu, and Y. Cheng, "Drio: Robust radar-inertial odometry in dynamic environments," *IEEE Robotics and Automation Letters*, 2023.
- [6] C. Zhang, X. Zhang, X. Yue, M. Lao, T. Jiang, J. Wang, F. Zhang, and L. Chen, "Pd-refiner: An underlying surface inheritance refiner with adaptive edge-aware supervision for point cloud denoising," in *ACM Multimedia 2024*, 2024.
- [7] Y. Song, M. Zadan, K. Misra, Z. Li, J. Wang, C. Majidi, and S. Kumar, "Navigating soft robots through wireless heating," in *2023 IEEE International Conference on Robotics and Automation (ICRA)*, 2023, pp. 2598–2605.
- [8] K. Johnson, Z. Englhardt, V. Arroyos, D. Yin, S. Patel, and V. Iyer, *MilliMobile: An Autonomous Battery-free Wireless Microrobot*. New York, NY, USA: Association for Computing Machinery, 2023.
- [9] J. Wang, Y. Song, M. Zadan, Y. Shen, V. Chen, C. Majidi, and S. Kumar, *Wireless Actuation for Soft Electronics-free Robots*. New York, NY, USA: Association for Computing Machinery, 2023.
- [10] S. Pruthi, "Wireless robotics: A history, an overview, and the need for standardization," *Wirel. Pers. Commun.*, vol. 64, no. 3, p. 597–609, jun 2012.
- [11] Y. Wu, G. Guo, G. Tian, and W. Liu, "A model with leaf area index and trunk diameter for lorawan radio propagation in eastern china mixed forest," *Journal of Sensors*, vol. 2020, pp. 1–16, 2020.
- [12] A. Gadre, F. Yi, A. Rowe, B. Iannucci, and S. Kumar, "Quick (and dirty) aggregate queries on low-power wans," in *2020 19th ACM/IEEE International Conference on Information Processing in Sensor Networks (IPSN)*, 2020, pp. 277–288.
- [13] C. Li and Z. Cao, "Lora networking techniques for large-scale and long-term iot: A down-to-top survey," *ACM Comput. Surv.*, vol. 55, no. 3, feb 2022.
- [14] A. Balanuta, N. Pereira, S. Kumar, and A. Rowe, "A cloud-optimized link layer for low-power wide-area networks," in *Proceedings of the 18th International Conference on Mobile Systems, Applications, and Services*, 2020, pp. 247–259.
- [15] J. Petajajarvi, K. Mikhaylov, A. Roivainen, T. Hanninen, and M. Petässalo, "On the coverage of lpwans: range evaluation and channel attenuation model for lora technology," in *2015 14th international conference on its telecommunications (its)*. IEEE, 2015, pp. 55–59.
- [16] E. Díaz-Caballero, A. Belenguer, H. Esteban, V. E. Boria, C. Bachiller, and J. V. Morro, "Analysis and design of passive microwave components in substrate integrated waveguide technology," in *2015 IEEE MTT-S International Conference on Numerical Electromagnetic and Multiphysics Modeling and Optimization (NEMO)*, 2015, pp. 1–3.
- [17] R. Syms, T. Tate, and R. Bellerby, "Low-loss near-infrared passive optical waveguide components formed by electron beam irradiation of silica-on-silicon," *Journal of Lightwave Technology*, vol. 13, no. 8, pp. 1745–1749, 1995.
- [18] J. Chan, C. Zheng, and X. Zhou, "3d printing your wireless coverage," in *Proceedings of the 2nd International Workshop on Hot Topics in Wireless*, ser. HotWireless '15. New York, NY, USA: Association for Computing Machinery, 2015, p. 1–5.
- [19] X. Xiong, J. Chan, E. Yu, N. Kumari, A. A. Sani, C. Zheng, and X. Zhou, "Customizing indoor wireless coverage via 3d-fabricated reflectors," ser. BuildSys '17. New York, NY, USA: Association for Computing Machinery, 2017.
- [20] M. Dunna, C. Zhang, D. Sievenpiper, and D. Bharadia, "Scattermimo: Enabling virtual mimo with smart surfaces," in *Proceedings of the 26th Annual International Conference on Mobile Computing and Networking*, ser. MobiCom '20. New York, NY, USA: Association for Computing Machinery, 2020.
- [21] X. Li, C. Feng, X. Wang, Y. Zhang, Y. Xie, and X. Chen, "RF-Bouncer: A programmable dual-band metasurface for sub-6 wireless networks," in *20th USENIX Symposium on Networked Systems Design and Implementation (NSDI 23)*. Boston, MA: USENIX Association, Apr. 2023, pp. 389–404.
- [22] C. Feng, X. Li, Y. Zhang, X. Wang, L. Chang, F. Wang, X. Zhang, and X. Chen, "Rflens: metasurface-enabled beamforming for iot communication and sensing," in *Proceedings of the 27th Annual International Conference on Mobile Computing and Networking*, ser. MobiCom '21. New York, NY, USA: Association for Computing Machinery, 2021, p. 587–600.
- [23] A. Ali, A. Mitra, and B. Aïssa, "Metamaterials and metasurfaces: A review from the perspectives of materials, mechanisms and advanced metadevices," *Nanomaterials*, vol. 12, 2022.
- [24] M. Alibakhshikenari, E. M. Ali, M. Soruri, M. Dalarsson, M. Nasermoghadasi, B. S. Virdee, C. Stefanovic, A. Pietrenko-Dabrowska, S. Koziel, S. Szczepanski, and E. Limiti, "A comprehensive survey on antennas on-chip based on metamaterials, metasurface, and substrate integrated waveguide principles for millimeter-waves and terahertz integrated circuits and systems," *IEEE Access*, vol. 10, pp. 3668–3692, 2022.
- [25] L. H. Blumenschein, L. T. Gan, J. A. Fan, A. M. Okamura, and E. W. Hawkes, "A tip-extending soft robot enables reconfigurable and deployable antennas," *IEEE Robotics and Automation Letters*, vol. 3, no. 2, pp. 949–956, 2018.
- [26] J. Ou, M. Skouras, N. Vlavianos, F. Heibeck, C.-Y. Cheng, J. Peters, and H. Ishii, "aeromorph - heat-sealing inflatable shape-change materials for interaction design," ser. UIST '16. New York, NY, USA: Association for Computing Machinery, 2016, p. 121–132.
- [27] L. Yao, R. Niizyama, J. Ou, S. Follmer, C. Della Silva, and H. Ishii, "Pneui: Pneumatically actuated soft composite materials for shape changing interfaces," in *Proceedings of the 26th Annual ACM Symposium on User Interface Software and Technology*, ser. UIST '13. New York, NY, USA: Association for Computing Machinery, 2013, p. 13–22.
- [28] L.-K. Ma, Y. Zhang, Y. Liu, K. Zhou, and X. Tong, "Computational design and fabrication of soft pneumatic objects with desired deformations," *ACM Trans. Graph.*, vol. 36, no. 6, nov 2017.
- [29] J. Wang and A. Chortos, "Performance metrics for shape-morphing devices," *Nature Reviews Materials*, vol. 9, no. 10, pp. 738–751, 2024.
- [30] C. Harrison and S. E. Hudson, "Texture displays: A passive approach to tactile presentation," in *Proceedings of the SIGCHI Conference on Human Factors in Computing Systems*, ser. CHI '09. New York, NY, USA: Association for Computing Machinery, 2009, p. 2261–2264.
- [31] E. Sevinchan, I. Dincer, and H. Lang, "A review on thermal management methods for robots," *Applied Thermal Engineering*, vol. 140, pp. 799–813, 2018.
- [32] R. I. Zelaya, R. Ma, and W. Hu, "Towards 6g and beyond: Smarten everything with metamorphic surfaces," in *Proceedings of the 20th ACM Workshop on Hot Topics in Networks*, ser. HotNets '21. New York, NY, USA: Association for Computing Machinery, 2021, p. 155–162.
- [33] L. Chen, M. Weng, P. Zhou, L. Zhang, Z. Huang, and W. Zhang, "Multi-responsive actuators based on a graphene oxide composite: intelligent robot and bioinspired applications," *Nanoscale*, vol. 9, no. 28, pp. 9825–9833, 2017.
- [34] X. Yang, J. Sayono, and Y. Zhang, "Cubesense++: Smart environment sensing with interaction-powered corner reflector mechanisms," in *Proceedings of the 36th Annual ACM Symposium on User Interface Software and Technology*, ser. UIST '23. New York, NY, USA: Association for Computing Machinery, 2023.
- [35] Q. Wu and R. Zhang, "Intelligent reflecting surface enhanced wireless network via joint active and passive beamforming," *IEEE Transactions on Wireless Communications*, vol. 18, no. 11, pp. 5394–5409, 2019.
- [36] X. Tan, Z. Sun, D. Koutsoukolas, and J. M. Jornet, "Enabling indoor mobile millimeter-wave networks based on smart reflect-arrays," in *IEEE INFOCOM 2018-IEEE Conference on Computer Communications*. Buffalo, NY, USA: IEEE, 2018, pp. 270–278.
- [37] E. Basar, M. D. Renzo, J. de Rosny, M. Debbah, M.-S. Alouini, and R. Zhang, "Wireless communications through reconfigurable intelligent surfaces," 2019.
- [38] V. Arun and H. Balakrishnan, "RFocus: Beamforming using thousands of passive antennas," in *17th USENIX Symposium on Networked*

- Systems Design and Implementation (NSDI 20)*. Santa Clara, CA: USENIX Association, Feb. 2020, pp. 1047–1061.
- [39] K. W. Cho, M. H. Mazaheri, J. Gummesson, O. Abari, and K. Jamieson, “mmWall: A steerable, transfective metamaterial surface for NextG mmWave networks,” in *20th USENIX Symposium on Networked Systems Design and Implementation (NSDI 23)*. Boston, MA: USENIX Association, Apr. 2023, pp. 1647–1665.
- [40] A. W.-L. Wong, S. L. Goh, M. K. Hasan, and S. Fattah, “Multi-hop and mesh for lora networks: Recent advancements, issues, and recommended applications,” *ACM Comput. Surv.*, vol. 56, no. 6, jan 2024.
- [41] K. Mekki, E. Bajic, F. Chaxel, and F. Meyer, “Overview of cellular lpwan technologies for iot deployment: Sigfox, lorawan, and nb-iot,” in *2018 ieee international conference on pervasive computing and communications workshops (percom workshops)*. IEEE, 2018, pp. 197–202.
- [42] C. Liu, R. He, R. Xu, R. Chen, J. Lv, W. Zhang, S. Wang, W. Li, W. Sun, and L. Li, “Measurement and analysis of lora transmission performance in subway station,” in *2022 IEEE 8th International Conference on Computer and Communications (ICCC)*, 2022, pp. 912–916.
- [43] M. Rahman and A. Saifullah, “Integrating low-power wide-area networks for enhanced scalability and extended coverage,” *IEEE/ACM Transactions on Networking*, vol. 28, no. 1, pp. 413–426, 2020.
- [44] M. I. Nashiruddin and A. Hidayati, “Coverage and capacity analysis of lora wan deployment for massive iot in urban and suburban scenario,” in *2019 5th International Conference on Science and Technology (ICST)*, vol. 1. IEEE, 2019, pp. 1–6.
- [45] S. Ravi, P. Zand, M. El Soussi, and M. Nabi, “Evaluation, modeling and optimization of coverage enhancement methods of nb-iot,” in *PIMRC’19*. IEEE, 2019, pp. 1–7.
- [46] H. Q. Pham, M. C. Pham, V. C. Trinh, P. L. Nguyen, and T. H. Nguyen, “A q-learning-based energy efficiency optimization in lora networks,” ser. SOICT ’23. New York, NY, USA: Association for Computing Machinery, 2023, p. 312–318.
- [47] J. Ou, M. Skouras, N. Vlavianos, F. Heibeck, C.-Y. Cheng, J. Peters, and H. Ishii, “Aeromorph - heat-sealing inflatable shape-change materials for interaction design,” in *Proceedings of the 29th Annual Symposium on User Interface Software and Technology*, ser. UIST ’16. New York, NY, USA: Association for Computing Machinery, 2016, p. 121–132.
- [48] T. Johnson, “Morphing air.” [Online]. Available: <https://www.tatej.net/morphing-air>
- [49] P. Beckmann and A. Spizzichino, *The scattering of electromagnetic waves from rough surfaces*, ser. The Artech House radar library. Norwood, MA: Artech House, 1987 - 1963.
- [50] R. Shen and Y. Ghasempour, *Scattering from Rough Surfaces in 100+ GHz Wireless Mobile Networks: From Theory to Experiments*. New York, NY, USA: Association for Computing Machinery, 2023.
- [51] H. Schantz, “Near field propagation law & a novel fundamental limit to antenna gain versus size,” in *2005 IEEE Antennas and Propagation Society International Symposium*, vol. 3A, 2005, pp. 237–240 vol. 3A.
- [52] J. A. Shaw, “Radiometry and the friis transmission equation,” *American journal of physics*, vol. 81, no. 1, pp. 33–37, 2013.
- [53] A. E. Fuhs, *Radar cross section lectures*. Monterey, California, Naval Postgraduate School, 1982.
- [54] D. Rigotti, A. Dorigato, and A. Pegoretti, “3d printable thermoplastic polyurethane blends with thermal energy storage/release capabilities,” *Materials Today Communications*, vol. 15, pp. 228–235, 2018.
- [55] K. Kim, S. Kim, T. Kim, W. Kim, and J. Lee, “Spray-coated liquid metal reflectors for transparent hydrogel atomic force microscope cantilevers,” *Journal of Microelectromechanical Systems*, vol. 25, no. 5, pp. 848–850, 2016.
- [56] S. H. Jeong, K. Hjort, and Z. Wu, “Tape transfer atomization patterning of liquid alloys for microfluidic stretchable wireless power transfer,” *Scientific reports*, vol. 5, no. 1, p. 8419, 2015.
- [57] M. D. Bartlett, A. Fassler, N. Kazem, E. J. Markvicka, P. Mandal, and C. Majidi, “Stretchable, high-k dielectric elastomers through liquid-metal inclusions,” *Advanced Materials*, vol. 28, 2016.
- [58] W. C. Jakes and D. C. Cox, *Microwave Mobile Communications*. Milwaukee, Wisconsin, USA: Wiley-IEEE Press, 1994.
- [59] C. Li, H. Guo, S. Tong, X. Zeng, Z. Cao, M. Zhang, Q. Yan, L. Xiao, J. Wang, and Y. Liu, “Nelora: Towards ultra-low snr lora communication with neural-enhanced demodulation,” in *Proceedings of the 19th ACM Conference on Embedded Networked Sensor Systems*, ser. SenSys ’21. New York, NY, USA: Association for Computing Machinery, 2021, p. 56–68.
- [60] A. Dongare, R. Narayanan, A. Gadre, A. Luong, A. Balanuta, S. Kumar, B. Iannucci, and A. Rowe, “Charm: Exploiting geographical diversity through coherent combining in low-power wide-area networks,” in *2018 17th ACM/IEEE International Conference on Information Processing in Sensor Networks (IPSN)*, 2018, pp. 60–71.
- [61] A. Gadre, R. Narayanan, A. Luong, A. Rowe, B. Iannucci, and S. Kumar, “Frequency configuration for Low-Power Wide-Area networks in a heartbeat,” in *17th USENIX Symposium on Networked Systems Design and Implementation (NSDI 20)*. Santa Clara, CA: USENIX Association, Feb. 2020, pp. 339–352.